https://doi.org/10.5194/egusphere-2026-3659
Preprint. Discussion started: 26 June 2026

Ditches, microtopographical hotspots and hot moments drive greenhouse gas emissions from a clear-felled conifer plantation on an organic soil

Ben Keane[1], Emanuel Blei[2], Simon Gibson-Poole[3], Phil Ineson[4], James I. L. Morison[5], Mike Perks[6], Elena Vanguelova[5], Matt Wilkinson[5], Mathew Williams[7], Georgios Xenakis[6], Sirwan Yamulki[5], Sylvia Toet[4]

[1]Department of Environment and Geography, University of York, York, UK, YO10 5DD
[2]The Dot Collective, Southwark, 70 Colombo Street, London, UK, SE1 8DP
[3]SRUC, Peter Wilson Building, Kings Buildings, Edinburgh, UK, EH9 3JG
[4]Department of Biology, University of York, York, UK, YO10 5DD
[5]Forest Research, Alice Holt Lodge, Wrecclesham, Farnham, Surrey, UK, GU10 4LH
[6]Forest Research, Northern Research Station, Roslin, Midlothian, UK, EH25 9SY
[7]School of Geosciences, Grant Institute, King's Buildings, West Mains Road, Edinburgh, UK, EH9 3JW

Correspondence to: Ben Keane (james.benjamin.keane@gmail.com)

Abstract. In the United Kingdom (UK), forests on peaty gley, peaty podsol and deep peat soils contain ca. 50% of the total forest soil C stock (Vanguelova, 2015). Many such forests were planted in the 1970s and 80s and are due for harvest, raising the question: what is the greenhouse gas (GHG) balance after felling?

Typically, planted forests in the wetter UK uplands contain a network of ditches and ridge-with-furrows resulting in a complex mosaic of microtopographical features. Measuring GHG exchange from such a complex landscape is challenging; methane (CH_4) and nitrous oxide (N_2O) fluxes can vary greatly in both space and time, and ditches have been highlighted as potentially important GHG sources although they are challenging to measure.

We used a combination of flux measurement techniques to quantify GHG fluxes and identify the drivers from the key microtopographies (ridges, hollows, ditches) within an upland forest in northern England immediately after clear felling. We deployed manual flux chambers, a SkyLine2D automated chamber system and two eddy covariance towers to measure carbon dioxide (CO_2), CH_4, and N_2O for an intensive campaign of five weeks. We used remote sensing to estimate the proportions of microtopographies and upscaled fluxes from the chamber to the forest block scale. We investigated the contribution of brash to the GHG emissions of harvest through a litter addition experiment.

Cumulative flux estimates based on the different techniques and the GHGs measured varied considerably. We found that CO_2 fluxes did not differ between microtopographies but the needle litter in harvesting residues increased CO_2 emissions by ca. 33%. Soil moisture was an important driver of both CH_4 and N_2O fluxes. Ditches were the largest source of CH_4 fluxes, followed by hollows and then ridges. The opposite pattern was seen for N_2O fluxes, which were greatest from ridges and other drier areas within the landscape. Following heavy rainfall, emissions of all GHGs increased rapidly over the next 24 hours.

https://doi.org/10.5194/egusphere-2026-3659
Preprint. Discussion started: 26 June 2026

1 Introduction

Forests cover 30% of terrestrial ecosystems (Le Quéré et al., 2015) and organic soils store 500 GT C globally (Yu, 2012). During the 1970s and '80s, global forest expansion into drained peatlands saw ca. 140 000 km^2 (14 Mha) boreal and temperate land prepared for this purpose (Paavilainen and PäIväNen, 1995). In the United Kingdom (UK) alone, there are nearly 7000 km^2 of forests on peaty gley and peaty podsols, predominantly in upland areas; there are a further 2000 km^2 on deep peat soils, which cover 15% of the nation's land area and contain ca. 50% of the total soil C stock (Vanguelova, 2015). Preparing wet upland soils for afforestation in the past often involved draining soils to lower the water table, primarily through creation of a network of ditches. In the UK and Ireland, a further step in preparation for tree planting involved ploughing, leaving a repeating ridge-with-furrow characteristic to the landscape; trees were grown on the drier ridges with the wetter furrows or hollows left unplanted between (O'Carroll et al., 1981). The resulting forest landscape is a complex mosaic of microtopographical features, criss-crossed with ditches and other bodies of standing water.

As these plantations approach maturity, decisions about their future management must be taken, including considering the full greenhouse gas (GHG) balance implications. Factors to be decided include the method of harvesting and how to manage the land post-harvest, whether to re-plant or restore to any earlier open-habitat condition. The heterogeneity of the landscape and conditions resulting from harvest can result in substantial net emission of GHGs for a time. For example, removal of the dense forest canopy leads to much reduced CO_2 uptake; removing the trees also causes the water table to rise, providing anaerobic microsites conducive to both methane (CH_4) and nitrous oxide (N_2O) production (Zerva and Mencuccini, 2005; Wu et al., 2011); brash and other litter from the felled trees will decompose over the subsequent months, increasing levels of nitrate (NO_3) and organic C in the soil which can also lead to an increase in N_2O fluxes (Paavolainen and Smolander, 1998; Nodvin et al., 1988). In addition, organic soils are vulnerable to large C losses from decomposition and are particularly at risk from disturbance associated with harvesting. Further, to account fully for the GHG fluxes from such systems, all topographical features must be considered (Purvina et al.,. 2026; Yamulki et al., 2026). Peatland streams (Billett et al., 2015) and water bodies within ombrotrophic peatlands (Waddington and Roulet, 1996; Billett et al., 2015; Billett and Moore, 2008; Dinsmore and Billett, 2008) are known to be sources of CO_2 and CH_4. However, there is a lack of GHG data covering drainage ditches in these systems (Peacock et al., 2021) and even fewer studies have used automated approaches which can reveal important information regarding temporal dynamics of gas fluxes from these environments (e.g. Keane et al., 2021). It is essential therefore to understand the drivers of GHG emissions from harvested plantations in order to assess the long-term GHG balance of such forestry systems.

Several studies have investigated the effect of clear-fell ('clear cut') harvesting on GHG fluxes, with mixed findings, including increases (Tate et al., 2006), reductions (Zerva and Mencuccini, 2005) and no changes (Butnor et al., 2006; Takakai et al., 2008). A four-year study at the present site showed increases in soil CH_4 and N_2O emissions, but reduced soil CO_2 emissions following clear felling (Yamulki et al., 2021). Studies such as these assess the effects of clear-fell by comparison to unfelled areas, or 'before' and 'after' impact assessments. Whilst such studies, which utilise a relatively small number of replicated plots (< 12), have identified alterations to the GHG balance, it is very difficult to capture robustly the full effect over the complex mosaic of topography within the landscape. Due to the sporadic nature of CH_4 and N_2O production in particular, it is likely that GHG emissions are characterised by high spatial and temporal variability.

https://doi.org/10.5194/egusphere-2026-3659
Preprint. Discussion started: 26 June 2026

One of the biggest challenges to increasing the accuracy of GHG balance accounting in any landscape, is bridging the gap between top-down and bottom-up estimates. Attempts to scale up from chamber measurements often suffer from a low level of replication within the landscape (Budishchev et al., 2014). The aim of this study was to improve understanding of the importance of the spatial and temporal variability of fluxes contributing to the landscape scale flux, and to investigate their drivers to help us better manage these ecosystems to minimise GHG emissions. We used a unique combination of technologies to map the terrain of the landscape and measure GHGs from within it. Multispectral imaging, mounted on an unmanned aerial vehicle (UAV) was used to survey the study area and categorise the landscape to one of three major microtopographies: ridges, hollows and water bodies. We investigated the contribution of brash from felling to the landscape scale GHG flux through a litter addition experiment. Greenhouse gas flux measurements from an automated chamber system, SkyLine2D, were compared with eddy covariance data and upscaled using data from the UAV remote sensing. This integrated approached allowed an investigation into the driving process of GHG fluxes.

We hypothesised that we would see higher fluxes of CH_4 and N_2O from the hollows compared to the drier ridges. We also expected to see greater CH_4 emissions from the water bodies. We expected to see highest CO_2 fluxes from the ridges and also hypothesised that there would be an increase in emissions of CO_2 and N_2O from the collars with litter added.

https://doi.org/10.5194/egusphere-2026-3659
Preprint. Discussion started: 26 June 2026

2 Materials and Methods

2.1 Site description:

The measurements were carried out during late July and August 2015 in Harwood Forest, an extensive upland commercial conifer forest in Northumberland, northern England. The clear-felled site (55° 13' 55" N, 1° 59' 50" W) has a peaty-gley soil (histogleysol, WRB 2017) with an elevation of 280 m a.s.l. and the annual mean temperature and total rainfall were 8.2°C and 1224 mm averaged over 2015 and 2016. There was a 5° slope from the north and south parts of the area, down to a small stream which crossed the site (Figure 1), and the site had a dense network of ditches (approx. 25 m spacing) that were installed prior to initial planting of the moorland in 1958, when the site was originally ploughed, leaving it with ridge and furrow microtopography at approx. 2 m spacing. Prior to felling, the 42 ha area was predominately 58-year-old mature Sitka spruce (*Picea sitchensis*, Bong. Carr.) on 25.9 ha (77% of area, average stand density of 1450 stems ha^{-1}, and average yield class of 14.5 m^3 ha^{-1} y^{-1}), with Scots pine (*Pinus sylvestris*, L.), lodgepole pine (*Pinus contorta*, L.) and Norway spruce (*Picea abies* L.) on 3.2, 3.1 and 1.6 ha, respectively, and the remainder (8.2 ha) open ground areas. Felling by machine started in late January 2015 and was completed by early March 2015. Felling operations followed the standard practice of the Forestry Commission (Murgatroyd and Saunders, 2005) and only large timber (> 7 cm diameter) was removed from site. Tree tops and branches were left on site in rows as brash-mats and some of them were used by the harvesting machinery as flotation to prevent soil compaction. While the majority of the clear-felled area was to the south-west of the eddy covariance (EC) tower and in the prevailing wind direction, there were young Sitka spruce stands (11 years old, approx. 3.5 m tall at the time) on the north-west and north side and a mature Scots pine stand (approx. 18 m tall) to the south-east of the tower (Figure 2).

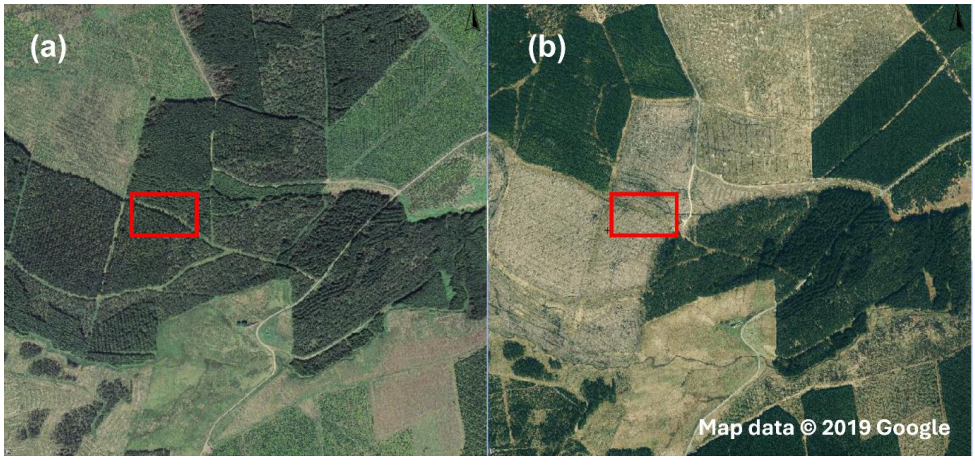

Figure 1. Aerial photography image of the study site before (a) and after (b) clear felling. The red square shows the main study site, shown in more detail in Figure 2a.

2.2 GIS surveying of microtopography of the site

The site was surveyed on 30th June 2015 using an unmanned multi-rotor aerial vehicle (UAV) and high-resolution imagery (two Canon A200 cameras) flying at an altitude of 115 metres to measure precisely the topography of

https://doi.org/10.5194/egusphere-2026-3659
Preprint. Discussion started: 26 June 2026

the site (Fig.2 a and b), prior to the measurement of GHG fluxes. The imagery was processed with AgiSoft Photoscan and ArcGIS, and was used to define the landscape according to three broad microtopography classifications: ridges, hollows and water bodies, which covered 43%, 46% and 11%, respectively, of the EC tower flux footprint, as determined from the standard footprint model (Kormann and Meixner, 2001).

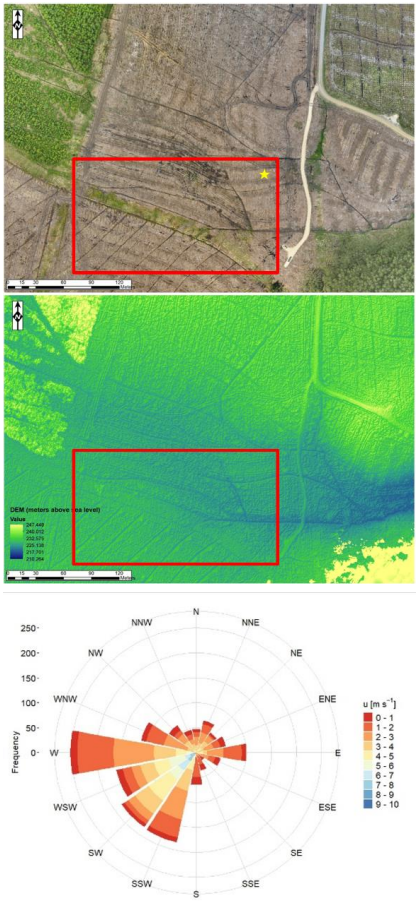

Figure 2. Overview of the Harwood Forest study site. The red rectangle illustrates the area in which the campaign focused its greenhouse gas (GHG) measurements. a) High resolution image of the clearfell study site taken using the UAV, with yellow star indicating eddy covariance tower position [I think!]; b) derived digital elevation model (colours indicating height above sea level, blue to yellows, low to high) c) wind rose illustrating the prevailing wind direction at the site during the campaign was from the SW.

https://doi.org/10.5194/egusphere-2026-3659
Preprint. Discussion started: 26 June 2026

2.3 Eddy covariance (EC) measurements:

One eddy covariance (EC) system was installed on top of a 6 m high lattice frame tower in April 2015, details of the set up are given in Xenakis et al. (2021), but briefly an open-path infra-red gas analyser (IRGA, model Li7500, LiCor Inc., Lincoln, NE, USA) that had been modified to enclose the optical path (Clement et al., 2009) sampled CO_2 and H_2O concentrations adjacent to a 3-axis sonic anemometer (CSAT-3, Campbell Scientific Ltd., Shepshed, Leics, UK), aligned to face into the predominant SW wind direction. This system is referred to as the semi-enclosed path EC system (SEP).

A second set of EC measurements were taken using closed path analysers, using a 3-axis sonic anemometer (USA-1, Metek GmbH, Elmshorm, Germany) mounted at the same height (6 m) on a 3 m pole above a 3 m tower section approximately 10 m due east of the SEP tower. The air was sampled adjacent to the anemometer at a flow rate of approximately 16 l min^{-1} using a dry scroll vacuum pump XDSi 35, Edwards, Burgess Hill, West Sussex, UK) and 37 m of unheated 3/8" od (6.4 mm id) diameter PTFE tube and drawn back to an instrument trailer for measurement of CH_4 mixing ratio by a cavity ring down spectroscopic fast methane analyser (FMA, model DLT-100, Los Gatos Research Inc., San Jose, CA, USA) and subsequently N_2O, CO_2 and H_2O mixing ratios by a quantum-cascade laser (QCL, model QC-TILDAS-76, Aerodyne Inc., Billerica, MA, USA). Gas analyser and sonic anemometer outputs were recorded at 10 Hz by custom made software using a Linux PC. The performance of both instruments was checked against N_2O, CH_4 and CO_2 mixture standards (BOC, UK) at two concentration levels (0.3, 1.8, 360 ppm and 0.6, 5, 1000 ppm respectively) before the start of the measurement campaign. This system is referred to as the closed path EC system (CP)

2.3.1 Data processing and quality checks

Half-hourly fluxes of energy (sensible and latent heat), momentum, CO_2, water vapour and CH_4 were calculated from the high frequency data using the EddyPro software package (v5.2, Li-Cor Inc.). Meteorological data were also averaged to half hourly periods and used for corrections of the calculated fluxes. Sonic anemometer velocity coordinates were corrected for tilt using a double axis rotation. Turbulent fluctuations were corrected using a block average de-trending algorithm and time-lag compensation was applied using the 'covariance maximization with a default value' method in EddyPro. The latter time-lag was calculated based on the length of the sampling tube and the flow rate of sampling. Fluxes measured by the SEP system were corrected for density fluctuations using the WPL method (Webb et al., 1980), but those for the CP system were not, due to the long tube length and as the gas analysers correct directly for water vapour content. Spectral corrections were applied to the calculated half hourly fluxes for low and high frequency losses using the analytical methods of Moncrieff et al. (1997) and Moncrieff et al. (2004), respectively, as implemented in the EddyPro software.

After processing and corrections, the quality of the fluxes was flagged using the Mauder and Foken (2004) system. Half hourly data were quality checked, and spikes were removed, and filtered to remove those below a friction velocity threshold (u^*_{TH}) using a custom-made R package (Xenakis, 2016) with the following steps. The poorest quality fluxes were first rejected (those flagged QC= 2). Then the data were u* filtered using a value of u^*_{TH} = 0.12 m s^{-1} determined using the methodology described by Papale et al. (2006) Subsequently, spikes occurring in the half hour values were removed using two methods. First, fluxes were grouped for each half hour and the 5% and 95% quantiles were calculated and half hourly fluxes below or above were considered a spike and removed. In the second method, the standard deviations (s.d.) of flux values, binned by day and night were calculated, and

https://doi.org/10.5194/egusphere-2026-3659
Preprint. Discussion started: 26 June 2026

any fluxes three times above or below the s.d. threshold for night-time and day-time fluxes, respectively were considered a spike and removed. Finally, some manual removal was necessary for points which were considered implausible. Spikes for sensible and latent heat were removed following the same two methods but with the reverse order, i.e., first based on standard deviation and then based on quantiles as this was found to remove fewer values.

Comparison of the half-hourly momentum, sensible heat and latent heat fluxes from the two EC systems showed that they agreed (after quality control) to within 2%, 10% and 6%, respectively (linear regression slopes).

2.4 Surface GHG flux measurements:

2.4.1 Automated flux measurements with the Skyline2D system:

Surface GHG fluxes were measured along a transect in the clear-fell area using SkyLine2D, an automated suspended chamber system designed and built at University of York. For a full description of the SkyLine2D system, see Keane *et al.* (2018). Briefly, the equipment comprised a single, clear cylindrical chamber (Perspex, inner diameter 20 cm, height 40 cm), suspended from a motorised trolley, programmed to traverse parallel ropes *ca*. 2 m above a transect. The system was automated to repeatedly visit pre-selected positions on the transect, where the chamber was lowered to sit on a collar to complete a gas flux measurement over a predetermined interval. Upon completion of the programmed chamber closure, the system raised the chamber and moved to the next programmed position to repeat the process.

A transect was chosen which captured the microtopography of the landscape (ridges, hollows and ditches) and was also upwind of the EC towers for the prevailing wind direction. Brash left from felling was cleared from the transect, which was *ca*. 30 m long and allowed for 27 measurement positions: 12 in hollows, 12 on ridges and 3 in water-filled drainage ditches. At each of the 24 terrestrial measurement points along the transect, a PVC collar (inner diameter 20 cm, height 10 cm) was inserted approximately 2 cm below the soil surface on 22nd July 2015. Fresh litter (needles and fine twigs) was collected from an adjacent stand of Sitka spruce of the same age as the recently felled trees. Half of the terrestrial measurement collars (ridges and hollows) were assigned at random to receive litter, which was applied by hand on 28th July at a rate typical of the fresh litter component of brash as calculated as from Cannell (1982). All measurements were made between 22nd July and 25th August 2015.

A closed-path IRGA in the motorised trolley was used to measure CO_2 flux in the chamber, (Li-8100, LiCor Inc.), and the outflow from the IRGA was circulated via polyethylene tubing (Bev-A-Line IV, Cole-Parmer, London UK; internal diameter 3 mm) sequentially to separate cavity ring-down (CRD) laser analysers for N_2O and CH_4 flux measurements (LGR isotopic N_2O analyser and LGR fast greenhouse gas analyser, Los Gatos Research, CA USA) housed in a small enclosure at one end of the SkyLine2D apparatus. Fluxes were calculated, using linear regression, as the rate of change of gas concentration, adjusted for chamber area, volume and temperature. CO_2 fluxes were calculated using the LiCor software and N_2O and CH_4 fluxes were calculated using SAS 9.4 (SAS Institute, NC USA). The chamber was programmed to close for five minutes with an interval of three minutes to purge the system, a measurement schedule which allowed each collar on the transect to be measured approximately every 270 minutes. A period of at least 30 seconds was allowed for mixing of the chamber headspace and regressions were performed on the subsequent three minutes.

https://doi.org/10.5194/egusphere-2026-3659
Preprint. Discussion started: 26 June 2026

High frequency (1 minute, averaged over 15 minutes) measurements of soil moisture and temperature at 5 cm depth were made in the centre of each programmed landing position using temperature (UA-001-64 Hoboware, Onset Corporation, MA USA) and soil moisture probes (S-SMDM00,5 Decagon Devices Inc, WA USA).

In the first step fluxes were quality controlled using the R^2 statistic of the CO_2 flux measurement, with values < 0.9 discarded. Measurements passing this threshold were then assessed using the output statistics from the regression calculation of N_2O and CH_4 fluxes; regressions with a P-value < 0.05 were accepted, while those that did not were treated as zero flux.

2.4.2 Manual soil GHG flux measurements

Soil CO_2, CH_4 and N_2O fluxes were measured using the manual static chamber method, with 8 square opaque PVC chambers (40 × 40 × 26 cm) temporarily placed on permanently installed frames, inserted tightly to a depth of about 3 cm (for details, see Yamulki et al. (2021)). Four flux chambers were positioned on either side of a water filled ditch with two near the ditch and the other two further away. During each measurement, a chamber was placed on top of the frames for one hour. Samples of the chamber headspace were taken by syringe at four intervals of 0, 20, 40 and 60 minutes and transferred to pre-evacuated 20 mL vials, as described in Yamulki et al. (2017). Concentrations of CO_2, CH_4 and N_2O were subsequently determined using a gas chromatograph ((GC), Clarus 500, PerkinElmer, UK) equipped with an electron capture detector and a flame ionisation detector for analysis of N_2O and CH_4 respectively. Detailed GC analysis, conditions, calibrations and concentration calculations have been reported by Yamulki et al. (2021). Fluxes were calculated from the linear increase of gas concentrations inside the chamber with time.

Soil CO_2 fluxes were measured from 25 wider additional locations using a portable IRGA and chamber system with permanently installed 20 cm diameter collars (Li-8100A gas analyser, and Li-8100-103 soil survey chamber, Li-Cor Inc.). Collars were randomly located across the site and fluxes were measured twice a week, for four weeks during the campaign. During each CO_2 flux measurement, soil temperature at 2 and 10 cm soil depth were measured by a thermometer (Hanna, Instrument, USA) and soil moisture at 6 cm depth by a moisture probe (Delta-T Devices Ltd, UK) from areas adjacent to each chamber.

Following normal micrometeorological convention, all fluxes are expressed here as positive away from the surface (sources, net efflux) and negative towards (sinks, net uptake). The net CO_2 flux is referred to as NEE, as usual.

2.5 Cumulative flux calculations

Cumulative fluxes for all three measurement methods (SkyLine2D, EC, manual chambers) were calculated using trapezoidal interpolation of the measured fluxes with no gap filling. Since all of the SkyLine2D and manual chambers were to the west of the EC towers, any EC fluxes from a wind direction < 180 degrees were filtered out form the cumulative calculations. GWP was calculated as CO_2 equivalents (CO_2-eq) over 100 years by multiplying the cumulative fluxes of each GHG by the factors in Forster *et al.,* (2021).

2.6 Soil chemistry sampling and analysis

Soil chemistry adjacent to the manual collars and SkyLine2D collars was sampled on 6th August. A 15 cm deep core was taken and analysed for inorganic N. Briefly, soils were extracted in 1 M potassium chloride (KCl) (1:4

https://doi.org/10.5194/egusphere-2026-3659
Preprint. Discussion started: 26 June 2026

ratio weight to volume) and analysed colourimetrically for ammonium (NH_4) and nitrate (NO_3) on a flow injection analyser.

3 Results

3.1 Meteorological conditions during the campaign

Air temperatures across the period ranged from a low of ca. 2 °C overnight 11- 12th August to a high of 25 °C in the afternoon of 13th August (Figure 3b). There were three sustained rainfall events, the first beginning on 26th July, lasting two days, the second occurred on 14th August and the third on 18th August (Figure 3d). Soil moisture levels responded in the 24 hours or so following these events. Soil moisture ranged from 0.45- 0.55 m^3 m^{-3} in the hollows and 0.36- 0.40 m^3 m^{-3} in the ridges (Figure 3e). Soil temperature did not vary as much as the air temperature and was similar between ridges, hollows and the water bodies (Fig. 3c).

https://doi.org/10.5194/egusphere-2026-3659
Preprint. Discussion started: 26 June 2026

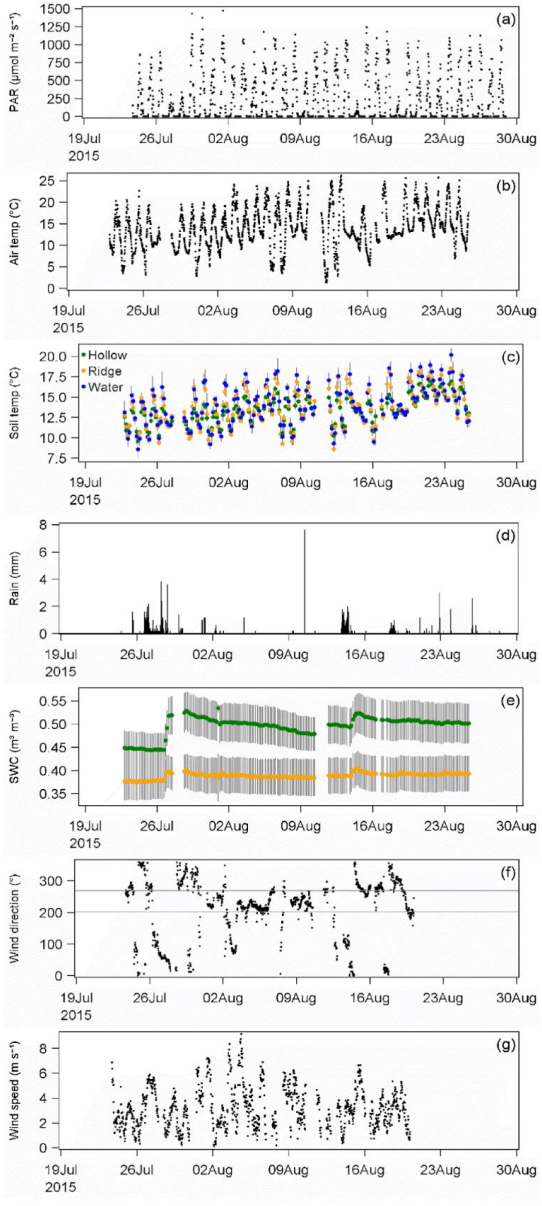

250

https://doi.org/10.5194/egusphere-2026-3659
Preprint. Discussion started: 26 June 2026

Figure 3. Time course of half-hourly meteorological data from the clear-fell site during the study period. Photosynthetically active radiation (PAR, panel a), air temperature (b), soil temperature at 5 cm depth from microtopographies within the SkyLine2D transect (c; yellow= ridges, green= hollows, blue= water), rainfall (d), volumetric soil water content from SkyLine2D microtopographies (SWC (e), yellow= ridges, green= hollows), wind direction, with horizontal lines indicating the direction of the SkyLine2D system relative to EC towers (f) and wind speed

3.2 Greenhouse gas fluxes

All CO_2 fluxes measured using the SkyLine2D chambers were positive, indicating net CO_2 emission, and a general trend of increasing magnitude was observed throughout the measurement campaign, which was reflected in the CO_2 fluxes measured using the manual survey chamber (Figure 4 a). Similarly, CH_4 fluxes measured using the SkyLine2D were all positive, with the largest emissions observed during the last 10 days of the campaign (Figure 4 c). Fluxes of CH_4 measured from the manual chambers were smaller with some evidence of oxidation, resulting in mean fluxes close to zero (Figure 4 b). The pattern of N_2O fluxes differed, as fluxes declined over the first half of the campaign to a low around 11th August, after which they increased again (Figure 4 e). While at the beginning of the campaign N_2O fluxes were similar in the SkyLine2D transect and manual chambers, during the second half of the measurement period manual N_2O fluxes were more than twice those measured using the SkyLine2D (Figure 4 e). EC CO_2 measurements consisted of both positive and negative fluxes, indicating that despite the felling of all the trees within the landscape, the EC tower footprint included some photosynthetic vegetation. Whilst the general sign of CO_2 fluxes measured with the two EC systems were consistent, half-hourly flux data from the two EC towers differed significantly ($t= 3.85$, $df= 570$, $p< 0.001$). Fluxes of CH_4 measured using the closed-path EC did not display any strong time-dependent patterns, but rather were more strongly affected by wind direction: the smallest fluxes were seen when the wind direction resulted in a footprint which included the SkyLine2D transect location (Figure 4 d, red symbols). Both positive and negative fluxes of N_2O , were observed (Figure 4 f), as found with CO_2 fluxes, and also with no clear pattern during the measurement campaign.

https://doi.org/10.5194/egusphere-2026-3659
Preprint. Discussion started: 26 June 2026

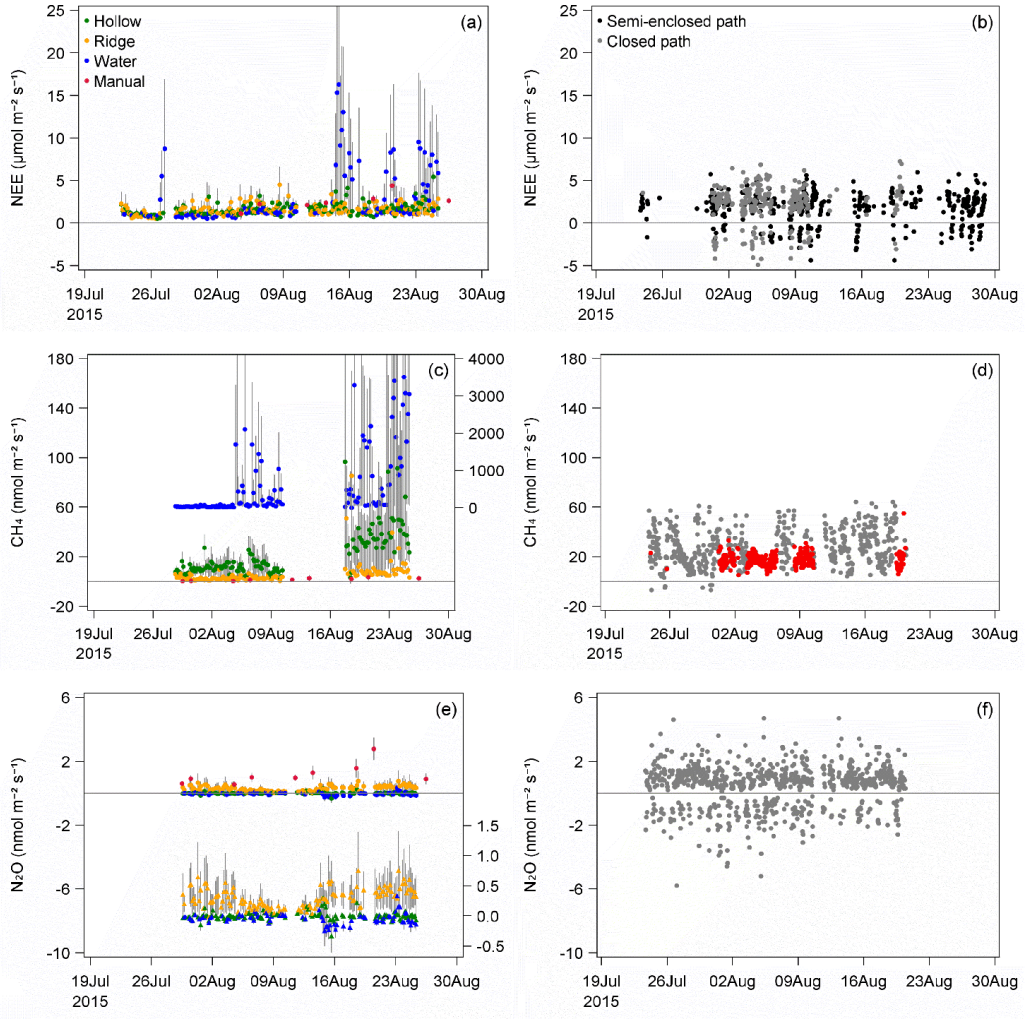

Figure 4. Time course of NEE (CO_2 flux, a and b), CH_4 flux (c and d) and N_2O (e and f) from the clear-felled forest site. Left hand column show SkyLine2D chamber transect data and right-hand side show EC data. Red symbols (d) indicate periods when the wind direction meant the EC footprint was measuring the area where SkyLine2D was located. SkyLine2D are grouped by microtopography (green= hollows, yellow= ridges, blue= water). Due to the higher CH_4 fluxes from the water, these are indicated on the right-hand axis of panel (c). N_2O fluxes are also expanded on the right-hand axis of (e) to better illustrate the differences between microtopographies. EC NEE data are grouped by two adjacent systems (black= semi enclosed path, grey= closed path).

3.3 Effect of microtopography, moisture and brash litter on GHG fluxes

Microtopography did not have a significant effect on CO_2 fluxes, but played an important role for both CH_4 and N_2O fluxes. The daily mean CH_4 flux measured along the SkyLine2D transect differed significantly between the

https://doi.org/10.5194/egusphere-2026-3659
Preprint. Discussion started: 26 June 2026

three topographies (F= 15.25, p< 0.01, Figure 5 a) with highest fluxes from the water bodies, the next highest from hollows and the lowest fluxes in the ridges. The largest emissions were in the days following persistent rainfall at the end of July and around 16th August (Figure 2 d). N_2O fluxes, on the other hand, were highest from ridges (F= 39.93, p< 0.001, Figure 5 b) compared to hollows and ditches and the only negative N_2O fluxes were observed from the ditches. The difference between N_2O fluxes from the microtopographies increased following periods of rainfall, where the soil moisture content of the ridges increased above 40% volumetric water content (VWC, Figure 3 e)

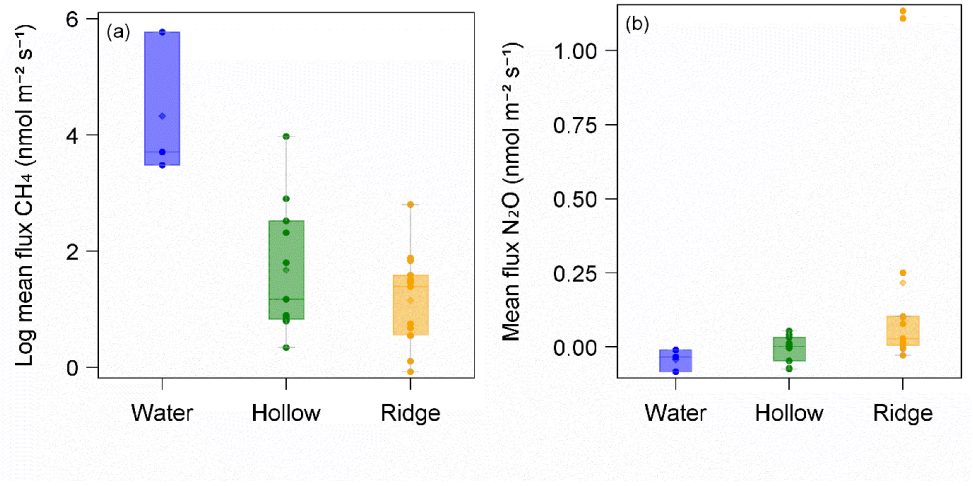

Figure 5. Whole campaign mean fluxes of CH_4 (panel (a)) and N_2O (panel b)) for the entire study period from each microtopography, measured using the SkyLine2D chamber transect. Diamond inside each box represents the microtopography mean, the solid horizontal line the median, the box is the interquartile range. Individual points represent individual chamber mean fluxes.Note the log scale for CH_4 fluxes.

Soil moisture differed significantly between not only the microtopographies of the SkyLine2D transect, but also the area in which the manual chambers were located (Figure 6 a). The hollows and ridges along the SkyLine2D transect had a mean soil moisture of 0.50 and 0.39 $m^3\ m^{-3}$ respectively, compared to ca. 0.25 $m^3\ m^{-3}$ in the manual chambers. Availability of inorganic N appeared to be related to soil moisture: in the wetter areas (hollows, and ridges), there was significantly more ammonium (NH_4) than in the drier manual chambers (Figure 6 b). In contrast, the hollows had the least nitrate (NO_3) available, which tended to increase in the drier ridges and was greatest in the manual chambers (Figure 6 c). This was reflected in the higher mean N_2O flux in the manual chambers (1.14 nmol $m^{-2}\ s^{-1}$) compared to 0.29 nmol $m^{-2}\ s^{-1}$ on the ridges in the SkyLine2D transect.

https://doi.org/10.5194/egusphere-2026-3659
Preprint. Discussion started: 26 June 2026

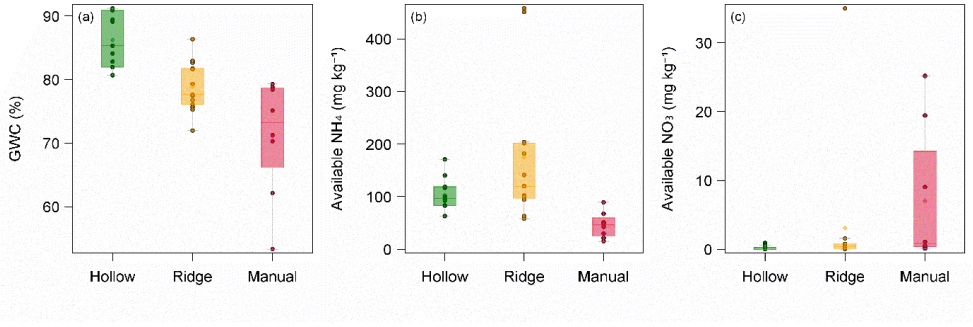

Figure 6. Variation in soil moisture and chemistry between the microtopographies of the SkyLine2D transect and the manual chamber locations. Properties shown are gravimetric soil moisture content (a), available ammonium (NH_4, (b)) and available nitrate (NO_3, (c)).

Although microtopography did not affect fluxes of CO_2 measured using the SkyLine2D, there were increased emissions from the ditches following rainfall which coincided with peaks in the CH_4 emissions. Addition of brash litter did increase cumulative CO_2 emissions however: the total flux of 5.62 ± 1.70 mol m^{-2} from the collars receiving brash (equivalent to 3.10 ± 0.27 g C m^{-2}) was ca. 33% greater than 4.23 ± 1.97 mol m^{-2} those without (equivalent to 2.31 ± 0.31 g C m^{-2}, Figure 7) and emissions appeared to be stimulated following the two major rainfall events on 27th July and 14th August. There was no significant effect of litter addition on the fluxes of N_2O and CH_4.

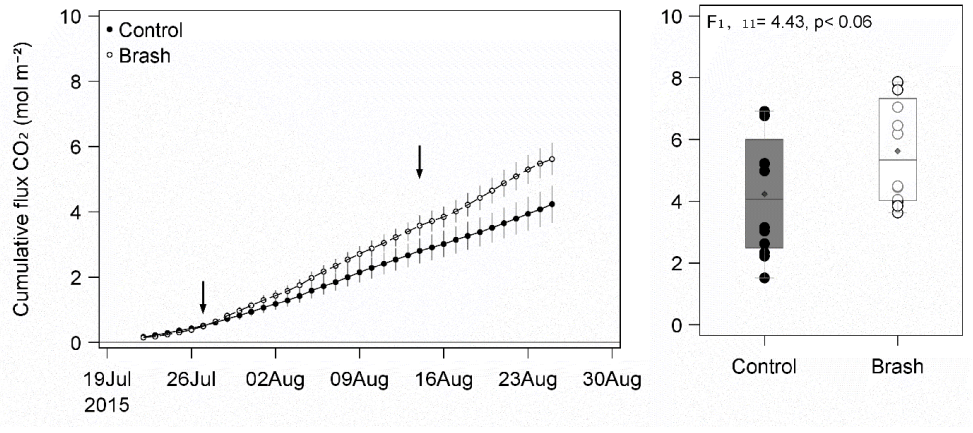

Figure 7. Effect of brash litter addition on soil CO_2 emissions, measured using the SkyLine2D chambers. Left hand panel denotes the cumulative CO_2 flux from collars calculated from the mean daily fluxes. Vertical arrows indicate periods of heavy rainfall which stimulated increased emissions from collars with added brash. Right hand panel shows the box plot of the final cumulative CO_2-C losses (add units?) from the collars at the end of the period. Values shown are means ± 1 SE (n= 12) for timeseries plot.

3.4 Diurnal analysis of GHG fluxes at this site and the influence of wind direction on EC data

CO_2 fluxes from both EC systems clearly showed uptake during the day (negative NEE values in Fig. 4b and lower positive mean values in Fig. 8), indicating that they were measuring some photosynthetic activity within

https://doi.org/10.5194/egusphere-2026-3659
Preprint. Discussion started: 26 June 2026

the footprint. Considering the data from both EC systems together, the largest (most positive) CO_2 fluxes at night were from a southerly direction (sectors centred between 130 and 210°, Figure 8).

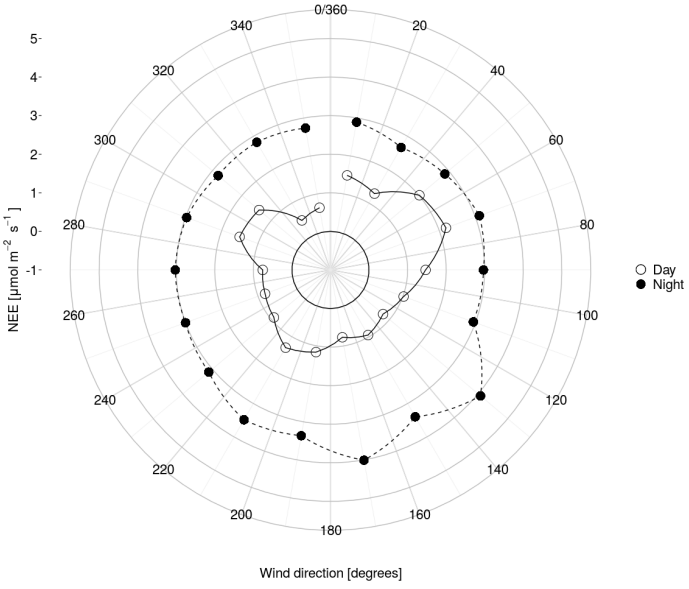

Figure 8. Distribution of half hourly NEE (µmol CO_2 m^{-2} s^{-1}) by wind direction, for each 20° increment, with distance from the centre of the wind rose indicating magnitude of flux (note: zero NEE is indicated by the black circle) ; shown separately for daytime and nighttime periods, measured from adjacent closed path (CP) and semi enclosed path (SEP) EC towers.

Fluxes of CH_4 and N_2O did not appear to differ between night and daytime (Figure 9). There was a strong directional influence on CH_4 fluxes, with the largest fluxes seen along an axis of 110° - 290°, which is a similar axis to the major drainage ditches for the site (Figure 10). The lowest CH_4 fluxes were seen from the north (340-360°) up the slope and the direction of the SkyLine2D system (180- 220°, Figure 9). Mean N_2O fluxes were close to net zero from all directions.

https://doi.org/10.5194/egusphere-2026-3659
Preprint. Discussion started: 26 June 2026

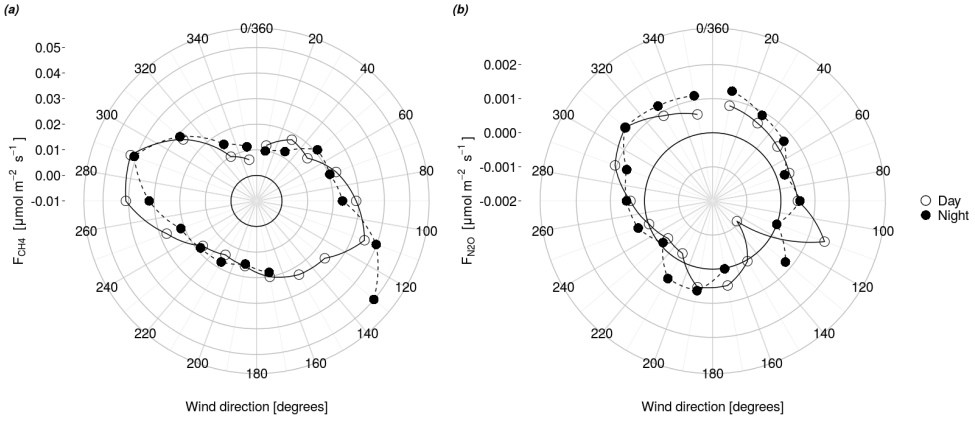

Figure 9. Distribution of CH_4 flux (left) and N_2O flux (right), by wind direction, for each 20° increment, with distance from the centre of the wind rose indicating magnitude of flux (note: zero is indicated by the black circle). Fluxes were measured using the closed path EC system, and are separated for day and nighttime periods.

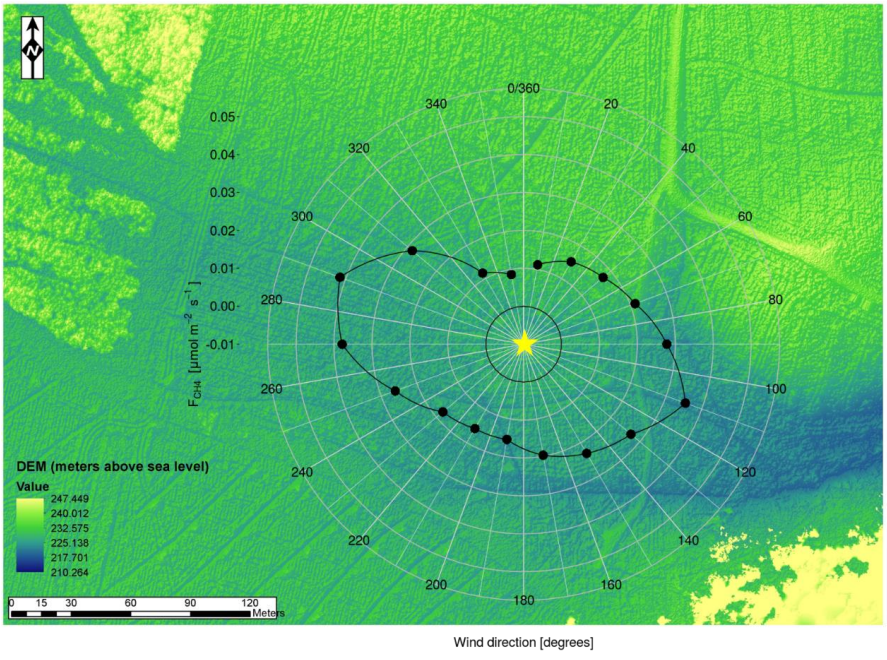

Figure 10. CH_4 fluxes measured using the closed path EC system (tower position indicated by yellow star) by wind direction superimposed on a high-resolution image of study area. Highest fluxes occurred when wind direction was along the axis of major drainage ditches.

https://doi.org/10.5194/egusphere-2026-3659
Preprint. Discussion started: 26 June 2026

3.5 Upscaling chamber flux measurements

Using the relative areas of the hollows, ridges and water bodies derived from the UAV imaging, the scaled-up cumulative CO_2 flux from the SkyLine2D transect was 4.35 ± 0.73 mol m^{-2}, 71% of that estimated from the CP EC system and 62% of that from the SEP system (Figure 11**Error! Reference source not found.** a). This was lower than the cumulative flux of 5.83 mol m^{-2} from the 25 manual CO_2 chamber measurements, which did not show systematic variations according to microtopography and were therefore not scaled. The manual total estimate was 95% of the CP EC system estimate and 83% of the SEP system estimate. The scaled-up CH_4 fluxes from the SkyLine2D transect were dominated by flux from the ditches, although they only covered 11% of the EC footprint. The SkyLine2D cumulative CH_4 flux of 127.30 mmol m^{-2} was nearly four times that of the CP EC system estimate of 32.51 mmol CH_4 m^{-2} (Figure 11b). The ditches' contribution to the SkyLine2D flux was very variable, with one of the ditch chambers emitting 500 times that of the other two.

When the data from this ditch (chamber 1) was omitted from the analysis, the estimated SkyLine2D cumulative CH_4 flux of 38.50 mmol m^{-2} was just 18% more than the EC estimate (Figure 11 c). In contrast to the similarity between the different methods' estimates of CO_2 flux, the estimated cumulative CH_4 flux from the 8 manual chambers was 3.98 mmol m^{-2}, ca. ten times lower than the estimate from the SkyLine2D transect without chamber 1 and that of the EC system. Ridges dominated the contribution to the cumulative SkyLine2D N_2O flux, which was 145 µmol N_2O m^{-2} compared to 941 µmol N_2O m^{-2} from the EC tower, 6.5 times smaller (Figure 11 d). The manual cumulative N_2O flux was higher, 4492 µmol N_2O m^{-2}, five times that of the EC and thirty times that of

https://doi.org/10.5194/egusphere-2026-3659
Preprint. Discussion started: 26 June 2026

365 the SkyLine2D upscaled fluxes. The manual chambers were the only measurement method which did not detect any negative fluxes.

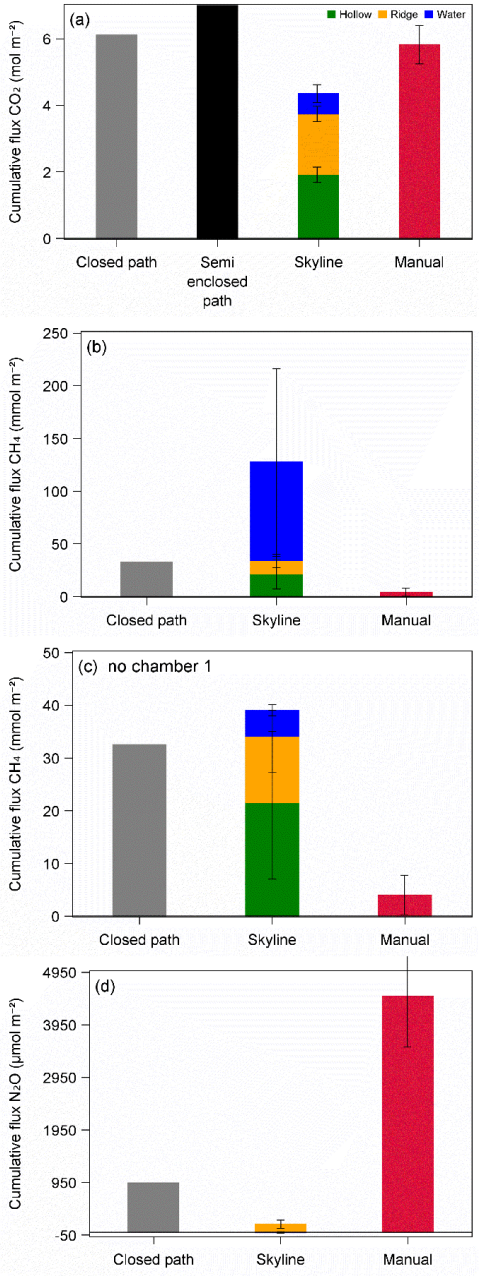

Figure 11. Cumulative fluxes of CO_2 (a), CH_4 (b and c) and N_2O (d) from the clear fell area from EC towers (closed path and semi enclosed path) and the SkyLine2D transect, with the scaled contribution of fluxes from the
370 **microtopographies (green= hollows, yellow= ridges, blue= water). CH_4 fluxes are shown with (b) and without chamber 1 (c), demonstrating the magnitude of the contribution of one ditch to the landscape scale flux of CH_4.**

https://doi.org/10.5194/egusphere-2026-3659
Preprint. Discussion started: 26 June 2026

Greenhouse gas balance

Depending on the measurement technique used, the contribution of each GHG to the total global warming potential (GWP) from the site in this summer measurement period varied (Table 1). Whilst all three techniques identified CO_2 as the highest GHG flux, the manual chambers estimated the N_2O flux to be the next largest contributor, as high as 19% of the total GHG flux, whilst the EC and SkyLine2D systems indicated that CH_4 was the next largest flux. The SkyLine2D transect data suggest that CH_4 might have contributed 33% of the total GHG flux, while EC measurements indicate that it was as low as 8%.

Table 1. Cumulative flux of each GHG expressed as global warming potential, GWP (Forster et al., 2021) measured using three different techniques. EC data are from the CP system. SkyLine2D data are upscaled based on the relative contributions of the three microtopographies and include chamber 1. Values are means (for SkyLine2D and manual chamber data) with standard errors in parentheses. Fluxes have been scaled to annual values by multiplying the mean daily cumulative by the number of days in the full year. Bold values indicate the proportion of each individual GHG's contribution to the total annual GHG flux.

Method	GWP (kg CO_2-eq m^{-2} y^{-1})		
	CO_2	CH_4	N_2O
EC	4.46; **88%**	0.42; **8%**	0.19; **4%**
SkyLine2D	3.17 (0.30); **67%**	1.64 (0.34); **33%**	0.03 (0.01); **0%**
Manual	4.25 (0.42); **80%**	0.05 (0.05); **1%**	0.89 (0.19); **19%**

https://doi.org/10.5194/egusphere-2026-3659
Preprint. Discussion started: 26 June 2026

4 Discussion

This work has provided important insights into the magnitude of GHG emissions following clear felling of a coniferous forest plantation on peaty-gley soil. We have highlighted important drivers and illustrated the temporal and spatial heterogeneity of GHG fluxes within this landscape. Using a unique combination of techniques: eddy covariance (EC), automated chambers (SkyLine2D) and manual gas flux chambers, we demonstrated the challenge of relying on GHG estimates from any single method.

4.1 Hotspots and hot moments of GHG fluxes

Microtopography influenced the fluxes of both CH_4 and N_2O at the fine spatial scale (e.g. along the SkyLine2D transect). However, the wider landscape scale also had a strong influence, with the manual chambers that were in a drier area of the site showing different flux magnitudes to those by the SkyLine2D and EC systems.

4.1.1 CH_4

Microtopography controlled CH_4 emissions across the site, with the lowest fluxes observed on the ridges, increasing with soil moisture in the hollows, but the largest source being the water bodies. This is to be expected as the source of CH_4 is expected to be anaerobic decay of organic material and sediments (Bubier et al., 1993). CH_4 fluxes in our study from hollows were routinely five times, and peaked at more than ten times, higher than the maximum reported in the 18 months following the felling of a Sitka spruce stand of similar age within the same forest (Ball et al., 2007). This may be due to the low frequency and replication of measurements made by Ball et al. (2007). We found that the terrestrial CH_4 emissions (from ridges and hollows) responded quickly to increasing soil moisture in the 24 hours following heavy and sustained rainfall events (26-7th July, 16th August), suggesting a rise in water table increased methanogenesis within the soil profile. Emissions from water bodies, however, were an order of magnitude larger than terrestrial CH_4 fluxes. Although it is known that the zone adjacent to drainage ditches can be large sources of CH_4 (Dinsmore et al., 2009), there have been few attempts to measure CH_4 emissions from the water surface of those ditches. In recent years, however, much more attention is being paid to these potentially important sources of GHGs (Silverthorn et al., 2025). Using the automated chamber system, SkyLine2D, we found emissions in excess of 3000 nmol m^{-2} s^{-1} from the small water bodies within our felled forest area, five times higher than fluxes measured from similar pools within peatlands elsewhere (Green et al., 2018). Although the measurements in this study were only for one summer month, if scaled to an annual flux, this would exceed some of the largest estimates measured using manual floating chambers by a factor of two (Peacock et al., 2021).

Not only was variation at the fine spatial scale important to CH_4 emissions, but fluxes varied by several orders of magnitude in very short periods of time here- i.e. there were several 'hot moments' of CH_4 emissions. The largest fluxes reported here occurred following the previously mentioned rainfall events, though the response time from the waterbodies was about 24- 36 hours longer than the terrestrial increases following rainfall. We interpret these increases as due to increased turbulence caused by faster flow through the drainage ditches. It is important to note the difference in the CH_4 emissions between the 3 water bodies measured using SkyLine2D. Of the three water locations measured along the transect, chamber 1 was one of the main drainage ditches for the site. Discounting

https://doi.org/10.5194/egusphere-2026-3659
Preprint. Discussion started: 26 June 2026

fluxes from this collar reduced the cumulative CH_4 flux estimate by ca. 70%. Whilst every care was taken to avoid causing ebullition by slowly closing the chamber onto a floating collar, the increased air flow rate may have increased the degassing of both CH_4 and CO_2 from the ditch through turbulence of the water. The importance of drainage ditches to the landscape flux is also highlighted by the highest EC CH_4 fluxes being along the same axis as the major ditches.

4.1.2 N_2O

N_2O fluxes across the site varied between the topographical features, which also differed in their soil moisture levels. The hollows and ridges along the SkyLine2D transect had a mean soil moisture of 0.50 and 0.39 m^3 m^{-3} respectively, compared to ca. 0.25 m^3 m^{-3} in the manual chambers, measured at comparable depths. In the drier areas, soil NO_3 levels decreased from manual collars, to ridges with hollows having the lowest concentration; the opposite trend seen compared to NH_4. We suggest that the drier conditions of the manual chambers and the ridges were more conducive to nitrification of NH_4, leading to the build-up of NO_3. Following rainfall, increasing soil moisture led to greater anaerobic conditions in the soil facilitating the denitrification of the accumulated NO_3 and the production of N_2O, a process which has been described previously in agricultural soils (Krichels et al., 2019). Throughout the campaign the maximum N_2O effluxes measured using EC were around 2 - 4 nmol m^{-2} s^{-1}, approximately 40-80% of the peak emissions reported from a Swiss mixed species forest following rainfall events (Eugster et al., 2007) but 20 times the mean fluxes measured over a two month spring-early summer period from a standing forest on drained peatland in Finland (Pihlatie et al., 2010), where soil NO_3 was close to zero. Over the eighteen months after clear felling of a Sitka stand in the same forest as this study (Ball et al., 2007), fortnightly manual measurements of soil N_2O flux peaked at around 0.25 nmol m^{-2} s^{-1}, ca. ten times lower than fluxes measured by the EC system in this study but similar to the fluxes measured using SkyLine2D. The highest individual flux was 6.37 nmol N_2O m^{-2} s^{-1}, measured from a chamber on the 20th of August when some of the wettest conditions were encountered (soil moisture within that particular chamber was 0.58 m^3 m^{-3}). This is an order of magnitude greater than the maximum soil flux reported after clear felling in a similar forest (Zerva and Mencuccini, 2005) and highlights the 'hotspot' nature of N_2O emissions, a term used to describe both the spatial (e.g. Dinsmore et al., 2009) and temporal (e.g. Vankessel et al., 1993) heterogeneity of fluxes of this GHG. An important point to make when comparing the flux estimates between the different measurement techniques, is the influence of negative fluxes. Whilst the mean fluxes from the manual chambers were similar to the maximum flux from the EC system, all the manual measurements were positive. In contrast, 29% of the EC fluxes and 39% of the SkyLine2D fluxes were negative, an important component of the wider areal flux that was not detected by the manual chambers. Whilst it may be the case that the area measured using manual chambers did not take up any N_2O, it is unlikely that the manual chambers would detect negative fluxes: gas chromatography is ill-suited to measuring N_2O below ambient concentrations and therefore it is difficult to quantify a negative flux with this technique (Cowan et al., 2014).

4.1.3 CO_2

Carbon dioxide effluxes measured by the SkyLine2D system were not strongly affected by the microtopographical features. Overall, the EC measurements showed this clear-felled area was a strong CO_2 source. While there was

https://doi.org/10.5194/egusphere-2026-3659
Preprint. Discussion started: 26 June 2026

some photosynthetic uptake, these lowest NEE values occurred when the wind direction was from the intact forest at the margins, although this direction was infrequent (see Fig 2c) .

4.1.4 Effect of litter on GHG emissions

The other important controlling factor on the landscape CO_2 flux was the presence of brash. The litter addition experiment suggested that approximately 33% of the CO_2 emitted at the site was derived from the brash litter left after felling. A recent global meta-analysis of harvest effects on soil respiration reported an average increase of 6.9% across all forest types and climates where residue was retained (Yang et al., 2024). It is not surprising that the introduction of fresh organic material would stimulate CO_2 efflux: for example, initial increases in soil CO_2 efflux were found in areas where brash was left after thinning of a first rotation Sitka spruce stand in Ireland (Olajuyigbe et al., 2012). In addition, the larger components of brash such as treetops, branches and the stumps left behind were not sampled by either the SkyLine2D transect or the manual chambers, but their CO_2 effluxes as decomposition starts will have been a component in the EC-measured CO_2 flux. The legacy of brash may be long-lasting: in similar re-wetted forest areas in Ireland after clear felling of a single Sitka spruce rotation, brash windrows emitted more CO_2 than other vegetation microsites, not due to higher soil respiration (R_s), but because brash piles do not revegetate compared to the forest floor between brash piles (Rigney et al., 2018). Brash piles have also been shown to be larger sources of CH_4 compared to other microsites of clear-felled forest floor more than five years after clear felling (Rigney et al., 2018), though we found no evidence of short-term increases in CH_4 fluxes with the brash fine litter addition. The longer-term effects of brash on N_2O fluxes need to be considered, as well. Work from Hubbard Brook showed that 18 months to 2 years following felling, NO_3 spiked within the catchment from the mineralisation from litter (Nodvin et al., 1988). As we have demonstrated in this study, the levels of NO_3 seem to drive N_2O emissions, thus it is to be expected that in the months following this study, N_2O emissions may well have increased further.

4.2 Upscaling GHG fluxes and appropriate chamber measurement strategies

Due to the hotspot nature of GHGs, several studies have attempted to develop chamber measurement strategies to accurately capture the landscape scale flux (Turner et al., 2016; Budishchev et al., 2014). The upscaling of fluxes in the current study met with varying degrees of success. The cumulative fluxes of CO_2 measured using the SkyLine2D chamber transect were within 20% of the landscape scale estimate of the EC tower. The manual chambers which had been placed without stratification for the different microtopography, also estimated the CO_2 flux within 20% of the EC total. The fluxes of the more transient GHGs, CH_4 and N_2O were less well captured by the manual chambers. The upscaled SkyLine2D CH_4 flux did agree with the estimate from the EC tower remarkably well, if the chamber data from the flowing water-filled drainage ditch was omitted from the analysis, with the upscaling estimating the cumulative flux within 10% of the EC flux. However, when that chamber was included, CH_4 flux estimates from the SkyLine2D transect were tripled. The directional influence on the EC CH_4 data also suggested that the main drainage ditches were important CH_4 sources. This introduces a challenge for defining the landscape scale flux: it is clear that water bodies play an important role in CH_4 emissions, but there is considerable variation between those bodies. As water bodies were not included, the manual chamber-derived estimate of CH_4 flux was an order of magnitude below that from EC and SkyLine2D methods, and a key aspect of the landscape GHG flux was missed.

https://doi.org/10.5194/egusphere-2026-3659
Preprint. Discussion started: 26 June 2026

Similarly, N_2O fluxes differed greatly across the landscape. The estimated cumulative flux from SkyLine2D data was considerably lower than that of the EC tower. The manual chamber data revealed that the drier areas of the clear-felled area emitted more than 10 times the N_2O flux of the SkyLine2D area, with the result that the SkyLine2D estimate was lower than the EC tower. The manual chambers may overestimate, primarily from failing to capture the full range of soil moisture at the site and therefore missed any negative fluxes. Negative fluxes are likely to be seen in very wet areas, where total denitrification of N_2O to N_2 gas will occur (Elmi et al., 2005). They were also seen from the waterbodies measured by the SkyLine2D system, which is another shortcoming of the manual chamber measurement method. In order to develop a robust sampling strategy for measuring GHG fluxes with chambers, it is essential to understand the drivers of each gas. Only then can the location and timing of measurements give a representative estimate of the landscape scale flux.

4.3 Implications for managing GHG emissions at felling

This study has focused on the GHG emissions following the conventional clear felling of a Sitka spruce stand where only the main stems were removed. There, are, however, alternative felling strategies, such as whole tree harvesting (WTH) where the entire standing biomass other than the stumps is removed from the site. Long term, WTH can increase soil carbon (C) and nitrogen (N) stocks (Vanguelova et al., 2010), since decomposition of litter left behind at harvest can have a priming effect increasing decomposition of existing organic material; here we have demonstrated that litter also increase CO_2 emissions following felling, and there is also the possibility it will drive increased N_2O emissions. The potential of WTH to mitigate in situ GHG emissions compared to clear felling therefore warrants more work, although this would also need to consider whether litter removal would simply displace GHG emissions at the eventual site of litter decomposition.

Despite variation between techniques seen in this study, all techniques consistently showed that the initial GHG emissions following clear fell were large. If fluxes had remained at the rates measured with EC, then a simple extrapolation (Table 1) indicates that CO_2 losses alone would amount to ca. 12 t C in the first year, which would be several times greater than the 2- 4 t C per year estimated to be incurred during preparation (e.g. draining and ploughing) of this soil type in the first place (Hargreaves et al., 2003). Such an extrapolation would be oversimplistic, and a longer-term study at this site showed that the actual accumulated C loss in the first year post felling was ca. 7 t C (Xenakis et al., 2021).

Non-CO_2 GHGs were also important contributors to the GHG balance at this site following felling and should not be neglected when considering management options. For example, N_2O emissions in our study were reduced where the soil was wetter. This may suggest that raising the water table would be beneficial in this respect and there is previous work which would shows this may be effective (Liu et al., 2020). Raising the water table would likely involve blocking the drainage channels, which were the largest source of CH_4 in this study. However, the raised water table is likely to increase CH_4 emissions across the rest of the landscape as shown by Evans *et al.* (2021) and this study. Further, rewetting would render the land impractical for further forestry. Ultimately, management options will be limited by the future use of the land, particularly if replanting is to be pursued as has been the case at this study site.

https://doi.org/10.5194/egusphere-2026-3659
Preprint. Discussion started: 26 June 2026

5 Conclusions

While all methods identified the clear-fell area as a net source of CO_2, CH_4 and N_2O, the estimated contribution of each gas to the overall GHG balance was dependent on the measurement technique used. One consistency was that all three techniques identified CO_2 as the largest contributor to the total GHG flux. It was also clear that CH_4 was an important flux to consider, as this was identified as the next most important GHG by the two measurement techniques (EC and SkyLine2D) which sampled at high temporal resolution. The importance of automated or near-continuous measurements was highlighted in the failure of manual chambers to identify the hot moments of fluxes and should be accounted for in future sampling strategies. The standout conclusion from this study is that accurately quantifying GHG emissions from such a heterogenous landscape is a huge challenge. Stratification of chamber sampling is vital, but this can only be achieved with appropriate knowledge of the drivers of GHGs.

Data availability

Data are available at: https://doi.org/10.5281/zenodo.5082059 (Yamulki et al., 2021b) and through the Environmental Information Data Centre (https://eidc.ac.uk/).

Author contributions

Ben Keane (BK), Emanuel Blei (EB), Simon Gibson-Poole (SGP), Phil Ineson (PI), James Morison (JM), Mike Perks (MP), Elena Vanguelova (EV), Matt Wilkinson (MWk) Mat Williams (MWm), Georgios Xenakis (GX), Sirwan Yamulki (SY), Sylvia Toet (ST).

Conceptualisation: PI, JM, MP, MWm, SY, ST
Methodology: BK, SGP, PI, JM, MP, MWk, MWm, GX, SY, ST
Formal analysis: BK, SGP, GX, SY, ST
Investigation BK, EB, SGP, PI, JM, MP, EV, MWk, MWm, GX, SY, ST
Data Curation: BK, EB, SGP, GX, SY, ST
Writing - Original Draft: BK, JM, SY, ST
Writing - Review & Editing: BK, SGP, PI, JM, MP, MWk, GX, SY, ST
Visualization: BK, SGP, GX
Supervision: PI, JM, MP, ST
Project administration: MWm, MP, ST
Funding acquisition: PI, MWm, ST, MP, JM

Competing Interests

The authors declare that they have no conflict of interest.

Disclaimer

Copernicus Publications adds a standard disclaimer: “Copernicus Publications remains neutral with regard to jurisdictional claims made in the text, published maps, institutional affiliations, or any other geographical

https://doi.org/10.5194/egusphere-2026-3659
Preprint. Discussion started: 26 June 2026

representation in this paper. While Copernicus Publications makes every effort to include appropriate place names, the final responsibility lies with the authors. Views expressed in the text are those of the authors and do not necessarily reflect the views of the publisher."

Please feel free to add disclaimer text at your choice, if applicable.

Acknowledgements

We would like to thank Vladimir Krivtsov and Adam Ash for soil and vegetation sampling and analysis and the Forestry England staff who gave permission for the study in Harwood Forest.

Financial support

This work was funded by the National Environmental Research Council (NERC) Generating Regional Emissions Estimates with a Novel Hierarchy of Observations and Upscaled Simulation Experiments (GREENHOUSE) project (NE/K002538/1 to Sylvia Toet and Phil Ineson, NE/K002619/1 to Mat Williams and NE/K002619/1 to Forest Research). The project was also funded by the Forestry Commission and by a NERC Independent Research Fellowship (NE/B000190/1) to Ben Keane.

Review statement

The review statement will be added by Copernicus Publications listing the handling editor as well as all contributing referees according to their status anonymous or identified.

https://doi.org/10.5194/egusphere-2026-3659
Preprint. Discussion started: 26 June 2026

References

Ball, T., Smith, K. A., and Moncrieff, J. B.: Effect of stand age on greenhouse gas fluxes from a Sitka spruce *Picea sitchensis* (Bong.) Carr. chronosequence on a peaty gley soil, Global Change Biology, 13, 2128-2142, 10.1111/j.1365-2486.2007.01427.x, 2007.

Billett, M. F. and Moore, T. R.: Supersaturation and evasion of CO_2 and CH_4 in surface waters at Mer Bleue peatland, Canada, Hydrological Processes, 22, 2044-2054, 10.1002/hyp.6805, 2008.

Billett, M. F., Garnett, M. H., and Dinsmore, K. J.: Should aquatic CO_2 evasion be included in contemporary carbon budgets for peatland ecosystems? Ecosystems, 18, 471-480, 10.1007/s10021-014-9838-5, 2015.

Bubier, J., Costello, A., Moore, T. R., Roulet, N. T., and Savage, K.: Microtopography and methane flux in boreal peatlands, northern Ontario, Canada, Canadian Journal of Botany-Revue Canadienne De Botanique, 71, 1056-1063, 10.1139/b93-122, 1993.

Budishchev, A., Mi, Y., van Huissteden, J., Belelli-Marchesini, L., Schaepman-Strub, G., Parmentier, F. J. W., Fratini, G., Gallagher, A., Maximov, T. C., and Dolman, A. J.: Evaluation of a plot-scale methane emission model using eddy covariance observations and footprint modelling, Biogeosciences, 11, 4651-4664, 10.5194/bg-11-4651-2014, 2014.

Butnor, J. R., Johnsen, K. H., and Sanchez, F. G.: Whole-tree and forest floor removal from a loblolly pine plantation have no effect on forest floor CO_2 efflux 10 years after harvest, Forest Ecology and Management, 227, 89-95, 10.1016/j.foreco.2006.02.018, 2006.

Cannell, M. G. R.: World forest biomass and primary production data–Academic Press, London, 391pp, 1982.

Clement, R., Burba, G., Grelle, A., Anderson, D., and Moncrieff, J.: Improved trace gas flux estimation through IRGA sampling optimization, Agricultural And Forest Meteorology, 149, 623-638, 10.1016/j.agrformet.2008.10.008, 2009.

Cowan, N. J., Famulari, D., Levy, P. E., Anderson, M., Reay, D. S., and Skiba, U. M.: Investigating uptake of N_2O in agricultural soils using a high-precision dynamic chamber method, Atmospheric Measurement Techniques, 7, 4455-4462, 10.5194/amt-7-4455-2014, 2014.

Dinsmore, K. J. and Billett, M. F.: Continuous measurement and modeling of CO_2 losses from a peatland stream during stormflow events, Water Resources Research, 44, 11, 10.1029/2008wr007284, 2008.

Dinsmore, K. J., Skiba, U. M., Billett, M. F., Rees, R. M., and Drewer, J.: Spatial and temporal variability in CH_4 and N_2O fluxes from a Scottish ombrotrophic peatland: Implications for modelling and up-scaling, Soil Biology & Biochemistry, 41, 1315-1323, 10.1016/j.soilbio.2009.03.022, 2009.

https://doi.org/10.5194/egusphere-2026-3659
Preprint. Discussion started: 26 June 2026

Elmi, A. A., Astatkie, T., Madramootoo, C., Gordon, R., and Burton, D.: Assessment of denitrification gaseous end-products in the soil profile under two water table management practices using repeated measures analysis, Journal of Environmental Quality, 34, 446-454, 2005.

Eugster, W., Zeyer, K., Zeeman, M., Michna, P., Zingg, A., Buchmann, N., and Emmenegger, L.: Methodical study of nitrous oxide eddy covariance measurements using quantum cascade laser spectrometery over a Swiss forest, Biogeosciences, 4, 927-939, 10.5194/bg-4-927-2007, 2007.

Evans, C., Peacock, M., Baird, A., Artz, R., Burden, A., Callaghan, N., Chapman, P., Cooper, H., Coyle, M., Craig, E., Cumming, A., Dixon, S., Gauci, V., Grayson, R., Helfter, C., Heppell, C., Holden, J., Jones, D., Kaduk, J., Levy, P., Matthews, R., McNamara, N., Misselbrook, T., Oakley, S., Page, S., Rayment, M., Ridley, L., Stanley, K., Williamson, J., Worrall, F., and Morrison, R.: Overriding water table control on managed peatland greenhouse gas emissions, Nature, 593, 548-+, 10.1038/s41586-021-03523-1, 2021.

Forster, P., Storelvmo, T., Armour, K., Collins, W., Dufresne, J.-L., Frame, D., Lunt, D., Mauritsen, T., Palmer, M., and Watanabe, M.: The Earth's energy budget, climate feedbacks, and climate sensitivity, 2021.

Green, S. M., Baird, A. J., Evans, C. D., Peacock, M., Holden, J., Chapman, P. J., and Smart, R. P.: Methane and carbon dioxide fluxes from open and blocked ditches in a blanket bog, Plant and Soil, 424, 619-638, 10.1007/s11104-017-3543-z, 2018.

Hargreaves, K. J., Milne, R., and Cannell, M. G. R.: Carbon balance of afforested peatland in Scotland, Forestry, 76, 299-317, 10.1093/forestry/76.3.299, 2003.

Keane, B., Ineson, P., Vallack, H. W., Blei, E., Bentley, M., Howarth, S., McNamara, N. P., Rowe, R. L., Williams, M., and Toet, S.: Greenhouse gas emissions from the energy crop oilseed rape (*Brassica napus*); the role of photosynthetically active radiation in diurnal N_2O flux variation, Global Change Biology Bioenergy, 10, 306-319, 10.1111/gcbb.12491, 2018.

Keane, J. B., Toet, S., Ineson, P., Weslien, P., Stockdale, J. E., and Klemedtsson, L.: Carbon Dioxide and Methane Flux Response and Recovery From Drought in a Hemiboreal Ombrotrophic Fen, Frontiers in Earth Science, 8, 10.3389/feart.2020.562401, 2021.

Kormann, R. and Meixner, F.: An analytical footprint model for non-neutral stratification, Boundary-Layer Meteorology, 99, 207-224, 10.1023/A:1018991015119, 2001.

Krichels, A., DeLucia, E. H., Sanford, R., Chee-Sanford, J., and Yang, W. H.: Historical soil drainage mediates the response of soil greenhouse gas emissions to intense precipitation events, Biogeochemistry, 142, 425-442, 10.1007/s10533-019-00544-x, 2019.

Le Quéré, C., Moriarty, R., Andrew, R. M., Canadell, J. G., Sitch, S., Korsbakken, J. I., Friedlingstein, P., Peters, G. P., Andres, R. J., Boden, T. A., Houghton, R. A., House, J. I., Keeling, R. F., Tans, P., Arneth, A.,

https://doi.org/10.5194/egusphere-2026-3659
Preprint. Discussion started: 26 June 2026

Bakker, D. C. E., Barbero, L., Bopp, L., Chang, J., Chevallier, F., Chini, L. P., Ciais, P., Fader, M., Feely, R. A., Gkritzalis, T., Harris, I., Hauck, J., Ilyina, T., Jain, A. K., Kato, E., Kitidis, V., Goldewijk, K. K., Koven, C., Landschutzer, P., Lauvset, S. K., Lefevre, N., Lenton, A., Lima, I. D., Metzl, N., Millero, F., Munro, D. R., Murata, A., Nabel, J., Nakaoka, S., Nojiri, Y., O'Brien, K., Olsen, A., Ono, T., Perez, F. F., Pfeil, B., Pierrot, D., Poulter, B., Rehder, G., Rodenbeck, C., Saito, S., Schuster, U., Schwinger, J., Seferian, R., Steinhoff, T., Stocker, B. D., Sutton, A. J., Takahashi, T., Tilbrook, B., van der Laan-Luijkx, I. T., van der Werf, G. R., van Heuven, S., Vandemark, D., Viovy, N., Wiltshire, A., Zaehle, S., and Zeng, N.: Global Carbon Budget 2015, Earth System Science Data, 7, 349-396, 10.5194/essd-7-349-2015, 2015.

Liu, H., Wrage-Mönnig, N., and Lennartz, B.: Rewetting strategies to reduce nitrous oxide emissions from European peatlands, Communications Earth & Environment, 1, 10.1038/s43247-020-00017-2, 2020.

Mauder, M. and Foken, T.: Documentation and Instruction Manual of the Eddy Covariance Software Package TK2, 2004.

Moncrieff, J. B., Clement, R., Finnigan, J. J., and Meyers, T.: Averaging and de-trending. Handbook of Micrometeorology, in: Handbook of Micrometeorology: A Guide for Surface Flux Measurement and Analysis, edited by: Lee, X., Massman, W., and Law, B., Kluwer Academic Publishing, Dordrecht, Netherlands, 7-31, 2004.

Moncrieff, J. B., Massheder, J. M., deBruin, H., Elbers, J., Friborg, T., Heusinkveld, B., Kabat, P., Scott, S., Soegaard, H., and Verhoef, A.: A system to measure surface fluxes of momentum, sensible heat, water vapour and carbon dioxide, Journal of Hydrology, 188, 589-611, 1997.

Murgatroyd, I. and Saunders, C.: Protecting the environment during mechanised harvesting operations, 2005.

Nodvin, S. C., Driscoll, C. T., and Likens, G. E.: Soil processes and sulfate loss at the Hubbard-Brook experimental forest, Biogeochemistry, 5, 185-199, 10.1007/bf02180227, 1988.

O'Carroll, N., Carey, M. L., Hendrick, E., and Dillon, J.: The tunnel plough in peatland afforestation, Irish Forestry, 1981.

Olajuyigbe, S., Tobin, B., Saunders, M., and Nieuwenhuis, M.: Forest thinning and soil respiration in a Sitka spruce forest in Ireland, Agricultural and Forest Meteorology, 157, 86-95, 10.1016/j.agrformet.2012.01.016, 2012.

Paavilainen, E. and Päivänen, J.: Peatland forestry: ecology and principles, Springer Science & Business Media1995.

Paavolainen, L. and Smolander, A.: Nitrification and denitrification in soil from a clear-cut Norway spruce (*Picea abies*) stand, Soil Biology and Biochemistry, 30, 775-781, 10.1016/s0038-0717(97)00165-x, 1998.

https://doi.org/10.5194/egusphere-2026-3659
Preprint. Discussion started: 26 June 2026

690 Papale, D., Reichstein, M., Aubinet, M., Canfora, E., Bernhofer, C., Kutsch, W., Longdoz, B., Rambal, S., Valentini, R., Vesala, T., and Yakir, D.: Towards a standardized processing of net ecosystem exchange measured with eddy covariance technique: algorithms and uncertainty estimation, Biogeosciences, 3, 571-583, 10.5194/bg-3-571-2006, 2006.

Peacock, M., Audet, J., Bastviken, D., Futter, M., Gauci, Grinham, A., Harrison, J., Kent, M., Kosten, S.,
695 Lovelock, C., Veraart, A., and Evans, C.: Global importance of methane emissions from drainage ditches and canals, Environmental Research Letters, 16, 10.1088/1748-9326/abeb36, 2021.

Pihlatie, M. K., Kiese, R., Bruggemann, N., Butterbach-Bahl, K., Kieloaho, A. J., Laurila, T., Lohila, A., Mammarella, I., Minkkinen, K., Penttila, T., Schonborn, J., and Vesala, T.: Greenhouse gas fluxes in a drained peatland forest during spring frost-thaw event, Biogeosciences, 7, 1715-1727, 10.5194/bg-7-1715-2010, 2010.

700 Purvina, D., Bardule, A., Zvaigzne, Z. A., and Lazdins, A.: Effect of deep furrowing on methane fluxes in non-drained peatland forest clearcuts, Engineering For Rural Development, DOI: 10.22616/ERDev.2026.25.TF096, 2026.

Rigney, C., Wilson, D., Renou-Wilson, F., Muller, C., Moser, G., and Byrne, K. A.: Greenhouse gas emissions from two rewetted peatlands previously managed for forestry, Mires and Peat, 21, 23,
705 10.19189/MaP.2017.OMB.314, 2018.

Silverthorn, T., Audet, J., Evans, C., van der Knaap, J., Kosten, S., Paranaiba, J., Struik, Q., Webb, J., Wu, W., Yan, Z., and Peacock, M.: The importance of ditches and canals in global inland water CO_2 and N_2O budgets, Global Change Biology, 31, 10.1111/gcb.70079, 2025.

Takakai, F., Desyatkin, A. R., Lopez, C. M. L., Fedorov, A. N., Desyatkin, R. V., and Hatano, R.: Influence of
710 forest disturbance on CO_2, CH_4 and N_2O fluxes from larch forest soil in the permafrost taiga region of eastern Siberia, Soil Science and Plant Nutrition, 54, 938-949, 10.1111/j.1747-0765.2008.00309.x, 2008.

Tate, K. R., Ross, D. J., Scott, N. A., Rodda, N. J., Townsend, J. A., and Arnold, G. C.: Post-harvest patterns of carbon dioxide production, methane uptake and nitrous oxide production in a *Pinus radiata* D. Don plantation, Forest Ecology and Management, 228, 40-50, 10.1016/j.foreco.2006.02.023, 2006.

715 Turner, P. A., Griffis, T. J., Mulla, D. J., Baker, J. M., and Venterea, R. T.: A geostatistical approach to identify and mitigate agricultural nitrous oxide emission hotspots, Science of the Total Environment, 572, 442-449, 10.1016/j.scitotenv.2016.08.094, 2016.

Vanguelova, E.: Protection of British forest soils in a changing management and policy challenges, in, edited by: Gonzalez, A. A., and Bengotxea, N. G., Servicio Central de Publicaciones del Gobierno Vasco, San
720 Sebastien, 2015.

https://doi.org/10.5194/egusphere-2026-3659
Preprint. Discussion started: 26 June 2026

Vanguelova, E., Pitman, R., Luiro, J., and Helmisaari, H. S.: Long term effects of whole tree harvesting on soil carbon and nutrient sustainability in the UK, Biogeochemistry, 101, 43-59, 10.1007/s10533-010-9511-9, 2010.

Vankessel, C., Pennock, D. J., and Farrell, R. E.: Seasonal-variations in denitrification and nitrous-oxide evolution at the landscape scale, Soil Science Society of America Journal, 57, 988-995, 10.2136/sssaj1993.03615995005700040018x, 1993.

Waddington, J. M. and Roulet, N. T.: Atmosphere-wetland carbon exchanges: Scale dependency of CO_2 and CH_4 exchange on the developmental topography of a peatland, Global Biogeochemical Cycles, 10, 233-245, 10.1029/95gb03871, 1996.

Webb, E. K., Pearman, G. I., and Leuning, R.: Correction of flux measurements for density effects due to heat and water-vapor transfer, Quarterly Journal of the Royal Meteorological Society, 106, 85-100, 10.1002/qj.49710644707, 1980.

Wu, X., Brueggemann, N., Gasche, R., Papen, H., Willibald, G., and Butterbach-Bahl, K.: Long-term effects of clear-cutting and selective cutting on soil methane fluxes in a temperate spruce forest in southern Germany, Environmental Pollution, 159, 2467-2475, 10.1016/j.envpol.2011.06.025, 2011.

Xenakis, G.: FREddyPro: post-processing EddyPro full output file, R package version, 1, 2016.

Xenakis, G., Ash, A., Siebicke, L., Perks, M., and Morison, J.: Comparison of the carbon, water, and energy balances of mature stand and clear-fell stages in a British Sitka spruce forest and the impact of the 2018 drought, Agricultural And Forest Meteorology, 306, 10.1016/j.agrformet.2021.108437, 2021.

Yamulki, S. and Morison, J. I. L.: Annual greenhouse gas fluxes from a temperate deciduous oak forest floor, Forestry, 90, 541-552, 10.1093/forestry/cpx008, 2017.

Yamulki, S., Ferraretto, D., Clement, R., Forster, J., Brunt, J., and Morison, J.: Assessing the effects of micro-topography resulting from previous ground preparation on forest floor GHG fluxes, Heliyon, 12, 10.1016/j.heliyon.2026.e44996, 2026.

Yamulki, S., Forster, J., Xenakis, G., Ash, A., Brunt, J., Perks, M., and Morison, J. I. L.: Effects of clear-fell harvesting on soil CO_2, CH_4, and N_2O fluxes in an upland Sitka spruce stand in England, Biogeosciences, 18, 4227-4241, 10.5194/bg-18-4227-2021, 2021.

Yang, L., Zhang, H., Qin, J., Liu, X., and Mayer, M.: A global meta-analysis of forest harvesting effects on soil respiration, its components, and temperature sensitivity, Agricultural And Forest Meteorology, 358, 10.1016/j.agrformet.2024.110259, 2024.

Yu, Z. C.: Northern peatland carbon stocks and dynamics: a review, Biogeosciences, 9, 4071-4085, 10.5194/bg-9-4071-2012, 2012.

https://doi.org/10.5194/egusphere-2026-3659
Preprint. Discussion started: 26 June 2026

Zerva, A. and Mencuccini, M.: Short-term effects of clearfelling on soil CO_2, CH_4, and N_2O fluxes in a Sitka spruce plantation, Soil Biology & Biochemistry, 37, 2025-2036, 10.1016/j.soilbio.2005.03.004, 2005.

755